

Multiphoton dissociative ionization of molecular deuterium

Ting S. Luk and Charles K. Rhodes

*Laboratory for Atomic, Molecular, and Radiation Physics, Department of Physics, University of Illinois at Chicago,
P.O. Box 4348, Chicago, Illinois 60680*

(Received 25 May 1988)

The kinetic energy spectra of deuterium ions produced from D_2 arising from collision-free subpicosecond irradiation at 248 nm with intensities spanning the 10^{13} – 10^{16} -W/cm² range have been measured by time-of-flight analysis. The behaviors of the kinetic energy distributions of the fragments and the relative abundances of atomic (D^+) and molecular (D_2^+) ions reveal the presence of two mechanisms of multiphoton dissociative ionization. Calibration of the energy scale for D^+ is facilitated by comparison with He^{2+} . For intensities in the 10^{13} – 10^{15} -W/cm² region, intermediate three-photon resonances and the optical Stark shift play important roles. At an intensity $\sim 10^{16}$ W/cm², a direct transition from the molecular ground state to the dissociative ionic level appears as a significant channel. No evidence of direct double ionization was observed.

I. INTRODUCTION

Molecular hydrogen is among the most abundant materials in the universe,¹ occupies a central position in quantum chemistry, and has attracted extensive experimental and theoretical study concerning many aspects of its structure and interactions. In particular, processes causing dissociation and ionization of molecular hydrogen and deuterium, the former, a reaction of considerable astrophysical significance, have been the subject of investigation for over 50 years.²

In the main, studies of dissociative ionization examining the kinetic energy distributions of the fragments and the relative abundances of atomic and molecular ions have been performed with electron impact.^{3–7} These experiments provide valuable information concerning the energy dependence of the oscillator strength⁸ and the Franck-Condon factor governing the overlap corresponding to the transition from the initial bound state to the continuum. In certain cases, experiments involving vacuum ultraviolet radiation, which serves as a more selective means of excitation than the charged particle process, have been performed.^{8–14} The role of autoionizing states has been a special topic of interest in this past work and the experimental identification of these levels is now quite well established.^{6,8,14}

Dissociative ionization arising from multiphoton processes is the mechanism explored in the present study, one channel of which is represented by the reaction



An examination of the kinetic energy distributions and abundances of the fragments, in conjunction with known molecular data, enables an evaluation of the role of intermediate resonances and two-electron effects on the dynamics¹⁵ of such multiphoton amplitudes.

II. EXPERIMENTAL PROCEDURES

In these studies of molecular fragmentation, a subpicosecond 248-nm source¹⁶ was used to produce the exci-

tation in a small focal volume under collision-free conditions and the energies of the ions were measured with the time-of-flight technique.⁸ The range of intensity studied spanned the 10^{13} – 10^{16} -W/cm² region.

An accurate means for the determination of ion kinetic energies was required for these experiments. In the case of deuterium, it is convenient to utilize the small difference in the charge to mass ratio that distinguishes D^+ from He^{2+} in order to provide a calibration for the time-of-flight system. The determination of the energy scale involves the use of the flight time of He^{2+} ($M/q=2.0013$ amu/e) as a fiducial in establishing the arrival time of D^+ ($M/q=2.014$ amu) over a range of ionic kinetic energies. This procedure has enabled the energy scale to be defined with an absolute accuracy of ± 0.2 eV with an energy resolution of ~ 0.5 eV.

Since the resolution of the instrument is degraded by sources of temporal dispersion of the flight time, these effects have been systematically examined. The causes of temporal dispersion are (1) the electronic response of the ion detector, (2) the molecular thermal energy, (3) the finite spatial extent of the focal region, (4) the beam pointing stability of the laser, and (5) the space charge associated with the ionized material. It was determined experimentally that the effect of space charge was the dominant source of temporal dispersion.

The influence of space charge on the ionic trajectories can be understood in the following manner. Immediately after ionization of the neutral molecules in the focal volume, the electrons are swept away by the ambient extraction field leaving a localized cloud of mutually repelling ions. For example, ions located at the periphery of the focal region will experience an electrostatic force proportional to the volume of the ionized material and, consequently, will develop an increased kinetic energy. If this potential energy is fully converted to kinetic form before entry into the drift tube, an additional width $\Delta\tau$ in the ion arrival times arising from this repulsion can be shown to be both independent of the ion energy in the drift region and simply related to the corresponding initial particle kinetic energy U_0 according to

$$\Delta\tau = \frac{\sqrt{(8U_0M)}}{E} \quad (2)$$

in which M and E denote the ion mass and extraction field, respectively. As described below, this feature actually enables the spatial size of the ionized region to be deduced, provided that a suitable assumption is made concerning the geometrical shape of the ionized volume.

Incomplete conversion of the potential energy to kinetic motion before entering the drift region, however, leads to an expansion of the spatial extent of the ion packet during the drift phase. The width $\Delta\tau$ is then given by the resulting length of the ion distribution divided by the average velocity of the particles, a relation expressed by

$$\Delta\tau = (ATZecr_0)\sqrt{(\pi\rho/U)} \quad (3)$$

in which r_0 is the initial radius of the ionized region, U the ion kinetic energy, ρ the gas density, T the total flight time, c the speed of light, Ze the ionic charge, and A a known constant with the value of 1.83×10^6 in c.g.s. units. Since the quantity T scales as $U^{-1/2}$, we have the simple overall relation

$$\Delta\tau U \simeq K, \quad (4)$$

for an appropriate constant K .

The experimental data support the relationship expressed by Eq. (4). The temporal widths of the signals for Ar^+ and Ar^{2+} , measured with the conditions described in the caption, are shown plotted versus $1/U$ in Fig. 1. The energy U was varied by the application of a potential

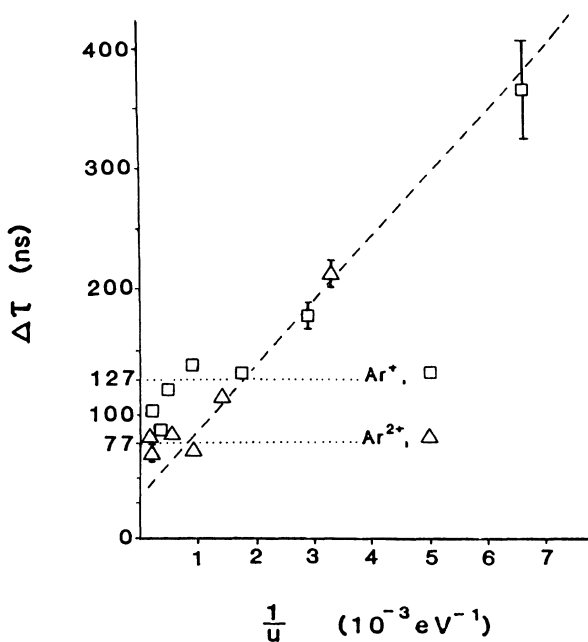


FIG. 1. Time-of-flight width $\Delta\tau$ for Ar ions at 10% maximum signal amplitude plotted vs the inverse of the total ion energy at a gas pressure of $\sim 10^{-6}$ Torr. These data were obtained with a 25-cm focal length lens.

that was *independent* of the ion extraction field. Although the linear behavior expected from Eq. (4) is present in the low-energy region ($U < 500$ eV), a plateau of essentially constant $\Delta\tau$ exists at higher energies. Significantly, the intercepts associated with the change in the slope depend upon the ionic charge state, with Ar^{2+} being below Ar^+ .

For the plateau, the width $\Delta\tau$ is determined by the nearly complete conversion of the potential energy into particle velocity. From Eq. (2), the measured widths for Ar^+ and Ar^{2+} correspond to kinetic energies of $\simeq 0.5$ eV and 0.09 eV, respectively. These measurements also give, with the assumption of the spherical distribution of ionized material, approximate values for r_0 of 94 and 60 μm , respectively, for Ar^+ and Ar^{2+} . Significantly, it was also found that the relative ionic abundances derived from these spot sizes agreed qualitatively with the experimentally observed yields.

Conversely, for the low-energy regime in which the ions are allowed to drift relatively slowly, any residual potential energy causes the ion packet to enlarge significantly in the drift zone. From the linear region in Fig. 1, the potential energy causing this additional width is estimated to be $\simeq 10^{-2}$ eV, a value small in comparison to the kinetic energies stated above.

A specific case illustrates the experimental situation. Measurements of He^{2+} at a gas density of $\sim 10^{-8}$ Torr yield a measured temporal width of ~ 5 ns for the He^{2+} signal. This value is consistent with the convolution of the contribution arising from the response of the detector and the thermal distribution of velocities. When the gas density was raised to $\sim 10^{-7}$ Torr, the linewidth broadened to $\simeq 10$ ns. The additional 5 ns of broadening is attributed to the kinetic energy arising from the influence of the space charge. Using this result to estimate the focal spot size, a value of 32 μm for the diameter is obtained, a magnitude in reasonable agreement with the experimental optical configuration.

With knowledge of these instrumental factors, the molecular experiments described below were performed in a regime for which (1) the density was sufficiently low so that the space charge energy was small, and (2) the ion energy was sufficiently high so that the expansion of the ion packet was negligible.

III. EXPERIMENTAL RESULTS AND DISCUSSION

The measured quantities, studied as a function of peak intensity, were (1) the ratio of abundances of the atomic (D^+) and molecular (D_2^+) ions, and (2) the kinetic energy distribution of the D^+ ions. The experimental findings are shown in Figs. 2 and 3 for the ionic ratio and the energy distributions, respectively.

The behavior of the relative abundance illustrated in Fig. 2 is broadly characterized by three regions. They are (1) for the lower intensities studied, roughly equal abundances independent of intensity, (2) a monotonic increase in relative atomic abundance with increasing intensity, and (3) a constant and high atomic ion fractional abundance at the extremum of the intensity range ($\sim 10^{16}$ W/cm^2).

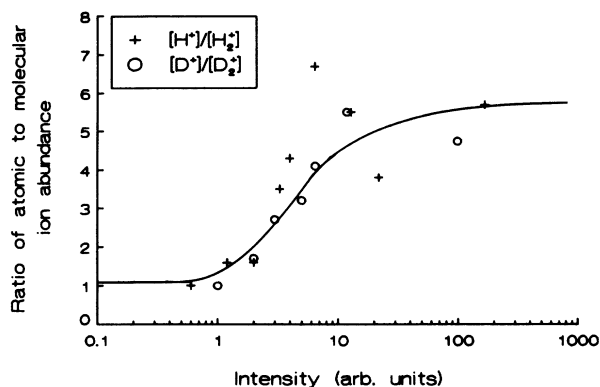


FIG. 2. Ratio of abundances of the atomic ($[H^+]/[D^+]$) and molecular ($[H_2^+]/[D_2^+]$) ions for hydrogen and deuterium plotted vs the 248-nm laser intensity.

Correspondingly, the main features of the kinetic energy spectra can be summarized as the following: (1) relatively few ions below 1 eV for the entire range of intensity investigated, (2) a prominent group of ions with energies in the 1–3-eV range at low intensity, (3) a second group of ions with energies spanning the 4–5-eV region appearing at moderate laser intensity, (4) at the highest intensity attainable ($\sim 10^{16}$ W/cm²), the observation of energetic ions up to a maximum energy of ~ 7 eV.

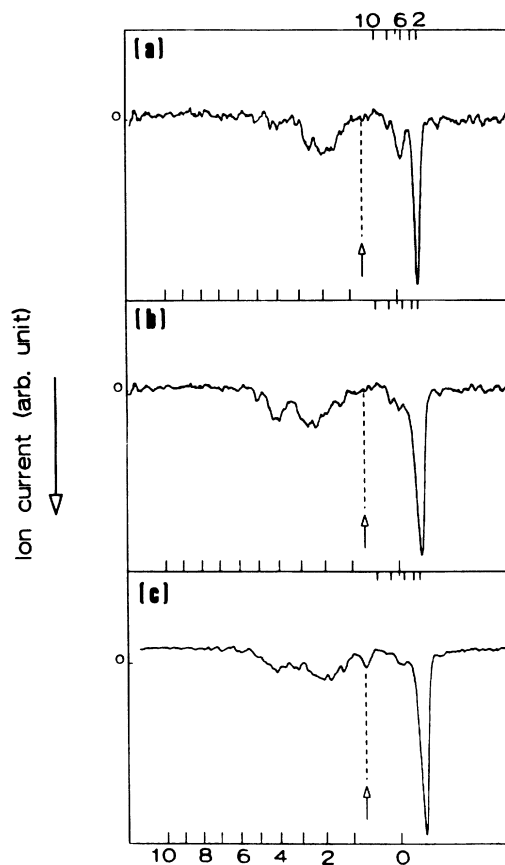
We now consider the D^+ kinetic energy spectrum observed at low intensity ($\sim 10^{13}$ – 10^{14} W/cm²). As an ansatz for this regime, we assume that the system will respond such that the lowest-order process available governs the main pathway for the production of the energetic ions. Therefore, the presence of near resonances for intermediate states would be expected to enhance the amplitudes of the significant channels. Specifically, several excited levels are present in molecular deuterium,^{17,18} at an energy, with respect to the ground state, corresponding almost exactly to three 248.5-nm quanta. Taking into account the thermal ($T=297$ K) rotational populations in the molecular ground level, the closest intermediate resonances for the most populous states are $D^1\Pi_u^+(v=5)$ and $D''^1\Pi_u^+(v=0)$ with energy detunings of 200 and 276 cm⁻¹, respectively. Although these states both have energies slightly below that corresponding to three quanta, even when the laser intensity is the minimum value used in these experiments ($\sim 10^{13}$ W/cm²), the optical Stark effect¹⁹ can be sufficiently large to bring some of these levels into resonance for a three-photon process. Once one of these states is excited, several channels are open. They are (1) predissociation, (2) radiative decay, (3) ionization of the neutral system through the absorption of an additional photon, and (4) dissociative ionization from the excited state through the absorption of more than one quantum.

With proper account for the difference in nuclear mass, the predissociative lifetimes of the D states of molecular deuterium are expected to be given approximately by the measured values for molecular hydrogen.²⁰ This gives a time on the order of a few picoseconds, a period somewhat longer than the duration of the ultraviolet pulse.

Dissociation of the states in the ~ 15 -eV region into the $D(2I)+D(1s)$ channel will produce ions in the ~ 1 -eV range through subsequent ionization of the atomic products. Therefore, we expect the observation of ions in the ~ 1 -eV energy range arising from irradiation at $\sim 10^{13}$ W/cm². Furthermore, since the dissociation and ionization steps are rapid in comparison to radiative decay of either the excited molecules or atoms,²¹ fluorescence should be insignificant.

In addition to low-energy particles, ions with kinetic energies in the 2–3-eV range are evident in the data shown in Fig. 3(a). These may arise from direct multiphoton dissociative ionization of the excited molecular level, namely, reaction (1) commencing from an excited

Kinetic energy away from the detector (eV)



Kinetic energy toward the detector (eV)

FIG. 3. Ion time-of-flight spectra of deuterium at (a) low ($\sim 10^{13}$ W/cm²), (b) moderate ($\sim 10^{15}$ W/cm²), and (c) high ($\sim 10^{16}$ W/cm²) 248-nm laser intensity. The gas pressure used in these experiments was $\sim 10^{-7}$ Torr. The arrows mark the positions corresponding to the arrival of the He^{2+} at the detector, points which enable the establishment of the energy scales for the deuterium ions. The intensity is sufficient to make the He^{2+} visible in (c). The lower scale represents the energy of ions moving toward the detector and the upper scale denotes the energy of the ions initially directed away from the detector.

state. Since a three-quantum process is required originally to produce the excited systems, any subsequent multi-quantum reaction involving less than three photons, beginning with an excited level such as the D state, is anticipated to have significant strength. With the ansatz that the vibronic wave function of the excited level is fully developed, an assumption based on the relatively short vibrational period of the system²² (~ 20 fs) in comparison to the ultraviolet pulse duration, the customary Franck-Condon factors can be used to represent the overlap corresponding to the transition. This procedure, known as the reflection approximation,²³ has been widely used in both single-photon^{10,11,24} and electron-impact^{7,8} studies. Using this method, the most probable dissociation energies are determined by the intersections of vertical lines with the $2p\sigma_u$ dissociate curve located at the internuclear positions corresponding to the maximum magnitude of the Franck-Condon factor. For the $D\ ^1\Pi_u^+(v=5)$ state, this gives ion energies of 2.2 and 3.1 eV for a two-photon dissociative ionization of the excited level, 4.0 and 5.2 eV for a corresponding three-quantum process, and likewise 6.7 and 9.3 eV for a four-photon amplitude. Furthermore, if the free electron wave function is approximated as a plane wave, in this energy range the electronic overlap is such that low dissociative energies are favored. Assuming that the lowest-order process dominates, the ions observed in Fig. 3(a) in the 2–3-eV range can be identified as arising from an overall five-photon dissociative ionization with a three-quantum resonant enhancement.

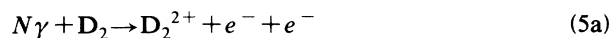
As the laser intensity is increased to a value of $\sim 10^{15}$ W/cm², a new group of deuterium ions appears in the 4–5-eV range. Several possible mechanisms could account for the production of these more energetic ions. They are (1) three-photon dissociative ionization from the molecular deuterium D -state manifold, a process, as noted above, that leads to ions in the 4.0–5.2-eV region, (2) three-photon dissociative ionization involving the $D''\ ^1\Pi_u^+(v=0)$ level dynamically stark shifted into resonance at an internuclear separation corresponding to ~ 1.05 Å, (3) excitation to the D_2^{2+} curve from the molecular D level by a six-quantum process at an internuclear distance of ~ 1.44 Å, and (4) production of ions from excited D_2^+ states at an internuclear separation of ~ 0.66 Å. In the latter two cases, (3) and (4), deuterium ions at ~ 9.3 eV associated with the $2p\sigma_u$ curve are expected in addition to the 4–5-eV component originating from the six-photon absorption. However, Fig. 3(b) clearly shows that the ions are concentrated in the region below 5.2 eV and virtually none are detected at higher kinetic energies. This experimental fact appears to rule out these two possibilities. However, if we again introduce the simplest ansatz that the lowest-order process has the greatest strength, cases (1) and (2), involving only three-photon amplitudes, emerge as the most likely processes generating the 4–5-eV group of ions. The participation of process (1), however, implies that an appreciable branching into that channel occurs even though the D state suffers a competitive loss into a two-photon channel and, furthermore, would be shifted out of resonance at this higher intensity. On this basis, we conclude that case

(1) is an unlikely candidate for the main channel producing the 4–5-eV ions. The remaining mechanism involves ion production through resonant enhancement of the dynamically Stark-shifted D'' state, case (2), at an internuclear separation of ~ 1.05 Å, a region exhibiting a large Franck-Condon overlap. Overall, this process involves a resonantly enhanced six-quantum amplitude.

The discussion above indicates that the molecular responses at $\sim 10^{13}$ and $\sim 10^{15}$ W/cm² are quite similar. Both involve resonant enhancement of a three-photon process, the former involving the D state while the latter occurs through the D'' level, both appropriately shifted in position by the radiative field.

At the maximum intensity used, $\sim 10^{16}$ W/cm², D^+ ions were detected up to an energy of ~ 7 eV, as shown in Fig. 3(c). It is expected that the contribution arising from the D'' state will decrease in this circumstance, since it will be shifted out of resonance at this intensity. However, higher-order direct processes are expected to become observable at sufficiently increased intensities and the group near 7 eV can be explained as originating by a direct dissociative ionization from the D_2 ground state $X\ ^1\Sigma_g^+$ to the $D_2^+ 2p\sigma_u$ level at an internuclear separation corresponding to the equilibrium value for the $X\ ^1\Sigma_g^+$ state. With the vertical energy of the strongly repulsive $2p\sigma_u$ level at ~ 32 eV and the $D^+ + D(1s)$ asymptote at ~ 18 eV, the total dissociative energy of 14 eV shared equally by the two nuclei accounts for the 7-eV energy observed. This reaction would involve a minimum of seven quanta, the naturally occurring next highest order process in relation to the five- and six-photon processes described above.

A direct amplitude for double ionization represented by



is allowed, in principle. For a vertical process,²⁵ D^+ ions with a kinetic energy of ~ 9.5 eV would be produced. Significantly, no ion signal was detected in that energy range, a finding which eliminates this process as an important channel for the experimental conditions studied in this work.

Finally, the relative abundances of the atomic and molecular ions are easily understood in the context of this description. A fraction of the molecules excited to the D state at low intensity can occupy weakly dissociating levels¹⁸ so that a subsequent single-photon ionization of the excited system can be effective in producing bound D_2^+ ions. Eventually, as the intensity increases, both the number of channels leading to dissociative ionization and the corresponding rates grow, so that the production of atomic ions eventually dominates.

IV. CONCLUSIONS

The behavior of multiquantum ionization of D_2 at 248 nm in the 10^{13} – 10^{16} -W/cm² range with subpicosecond ir-

radiation reveals the presence of two mechanisms of dissociative ionization. In the lower-intensity range between $\sim 10^{13}$ and $\sim 10^{15}$ W/cm², intermediate three-photon resonances and the optical Stark shift play important roles in determining the main channels of the molecular response. At an intensity of $\sim 10^{16}$ W/cm², a direct amplitude from the ground D₂ state to the dissociative ionic level appears as a significant channel. Finally, at the highest intensity used, D⁺ ions with energies ~ 9.5 eV, which would be the signature of direct double ionization, were not observed.

ACKNOWLEDGMENTS

The authors wish to acknowledge fruitful discussions with J. C. Solem and the technical assistance of P. Noel, R. Slagle, and J. R. Wright. This work was supported by the U.S. Office of Naval Research, the U.S. Air Force Office of Scientific Research, the Directed Energy Office and the Innovative Science and Technology Office of the Strategic Defense Initiative Organization, the Lawrence Livermore National Laboratory, and the National Science Foundation.

-
- ¹J. Michael Shull and Steven Beckwith, *Ann. Rev. Astron. Astrophys.* **20**, 163 (1982).
²H. S. W. Massey and E. H. S. Burhop, *Electronic and Ionic Impact Phenomena* (Oxford University Press, London, 1969), Vol. II.
³H. Dunn and L. J. Kieffer, *Phys. Rev.* **132**, 2109 (1962).
⁴A. Crowe and J. W. McConkey, *Phys. Rev. Lett.* **31**, 192 (1973).
⁵K. Köllmann, *J. Phys. B* **11**, 339 (1978).
⁶F. Pichou, R. I. Hall, M. Landau, and C. Schermann, *J. Phys. B* **16**, 2445 (1983).
⁷J. A. D. Stockdale, V. E. Anderson, A. E. Carter, and L. Deleanu, *J. Chem. Phys.* **63**, 3886 (1975).
⁸C. Backx, G. R. Wight, and M. J. Van der Wiel, *J. Phys. B* **9**, 315 (1976).
⁹G. R. Cook and P. H. Metzger, *J. Opt. Soc. Am.* **54**, 968 (1963).
¹⁰R. Browning and J. Fryar, *J. Phys. B* **6**, 364 (1973).
¹¹J. A. R. Samson and R. B. Cairns, *J. Opt. Soc. Am.* **55**, 1035 (1965).
¹²W. A. Chupka and J. Berkowitz, *J. Chem. Phys.* **51**, 4244 (1969).
¹³J. L. Gardner and J. A. R. Samson, *Phys. Rev. A* **12**, 1404 (1975).
¹⁴S. Strathdee and R. Browning, *J. Phys. B* **12**, 1789 (1979).
¹⁵L. J. Frasinski, K. Codling, P. Hatherly, J. Barr, I. N. Ross, and W. T. Toner, *Phys. Rev. Lett.* **58**, 2424 (1987).
¹⁶A. P. Schwarzenbach, T. S. Luk, I. A. McIntyre, U. Johann, A. McPherson, K. Boyer, and C. K. Rhodes, *Opt. Lett.* **11**, 499 (1986).
¹⁷A. Monfils, *J. Mol. Spectrosc.* **25**, 513 (1968).
¹⁸M. Rothschild, H. Egger, R. T. Hawkins, J. Bokor, H. Pummer, and C. K. Rhodes, *Phys. Rev. A* **23**, 206 (1981).
¹⁹T. Srinivasan, H. Egger, T. S. Luk, H. Pummer, and C. K. Rhodes, *IEEE J. Quantum Electron.* **QE-19**, 1874 (1983).
²⁰P. M. Dehmer and W. A. Chupka, *Chem. Phys. Lett.* **70**, 127 (1980).
²¹D. J. Kligler, J. Bokor, and C. K. Rhodes, *Phys. Rev. A* **21**, 607 (1980).
²²K. P. Huber and G. Herzberg, *Constants of Diatomic Molecules* (Van Nostrand, New York, 1979).
²³A. S. Coolidge, H. M. James, and R. D. Present, *J. Chem. Phys.* **4**, 193 (1936).
²⁴A. L. Ford, K. K. Docken, and A. Dalgarno, *Astrophys. J.* **195**, 819 (1975).
²⁵T. E. Sharp, *At. Data* **2**, 119 (1971).